ORGANIC LETTERS

2009
Vol. 11, No. 7
1639−1642

Functional Characterization of *ttmM* Unveils New Tautomycin Analogs and Insight into Tautomycin Biosynthesis and Activity

Jianhua Ju,[†,‡] Wenli Li,[†,‡] Qiuping Yuan,[§] Noel R. Peters,[§] F. Michael Hoffmann,[§] Scott R. Rajski,[‡] Hiroyuki Osada,[||] and Ben Shen[*,‡,⊥,#]

Division of Pharmaceutical Sciences, UW Paul P. Carbone Comprehensive Cancer Center Small Molecule Screening Facility, University of Wisconsin National Cooperative Drug Discovery Group, and, Department of Chemistry, University of Wisconsin, Madison, Wisconsin 53705-2222, and Antibiotics Laboratory, Chemical Biology Department, Advanced Science Institute, RIKEN, Wako-shi, Saitama 351-0198, Japan

bshen@pharmacy.wisc.edu

Received February 11, 2009

ABSTRACT

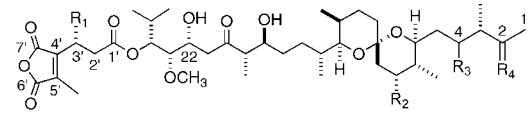

From *S. spiroverticillatus* wild-type: TTM, **1** (R_1 = OH, R_2 = H, R_3 = H , R_4 = O)

From Δ*ttmM* mutant SB6005:
- TTM M-1, **3** (R_1 = H, R_2 = H, R_3 = H , R_4 = O)
- TTM M-2, **4** (R_1 = H, R_2 = H, R_3 = OH , R_4 = —OH,H)
- TTM M-3, **5** (R_1 = H, R_2 = OH, R_3 = H , R_4 = O)

The biosynthetic gene cluster for tautomycin (TTM), a potent protein phosphatase (PP) inhibitor has recently been characterized. Inactivation of *ttmM*, which encodes a putative C3′ hydroxylase, afforded mutant SB6005 which accumulated three new 3′-deshydroxy TTM analogs, supporting the function of TtmM and the previously proposed linear pathway for TTM biosynthesis. Bioassays reveal the importance of the C3′ OH moiety in PP inhibition and that PP inhibition is not the exclusive mechanism driving TTM-induced cell death.

Tautomycin (TTM, **1**) and tautomycetin (TTN, **2**) are potent and selective inhibitors of the protein phosphatases (PPs) PP-1 and PP-2A.[1−3] The antitumor activity of both compounds has long been implied to result from PP inhibition. Importantly, apoptosis induction by **1** has been shown to be dependent on molecular features distinct from those attributed to PP inhibition, spurring interest in continued mechanistic investigations.[4] Both **1** and **2** exist as mixtures of interconverting anhydride and diacid forms in approximately a 5:4 ratio under neutral conditions (Figure 1).[5,6]

[†] These authors contributed equally to this contribution.
[‡] Division of Pharmaceutical Sciences.
[§] UW Paul P. Carbone Comprehensive Cancer Center Small Molecule Screening Facility.
[||] RIKEN.
[⊥] University of Wisconsin National Cooperative Drug Discovery Group.
[#] Department of Chemistry, University of Wisconsin.

(1) Honkanen, R. E.; Golden, T. *Curr. Med. Chem.* **2002**, *9*, 2055–2075.
(2) Mitsuhashi, S.; Matsuura, N.; Ubukata, M.; Oikawa, H.; Shima, H.; Kikuchi, K. *Biochem. Biophys. Res. Commun.* **2001**, *287*, 328–331.
(3) Oikawa, H. *Curr. Med. Chem.* **2002**, *9*, 2033–2054.
(4) Kawamura, T.; Matsuzawa, S.; Mizuno, Y.; Kikuchi, K.; Oikawa, H.; Oikawa, M.; Ubukata, M.; Ichihara, A. *Biochem. Pharmacol.* **1998**, *55*, 995–1003.
(5) Cheng, X. C.; Kihara, T.; Kusakabe, H.; Magae, J.; Kobayashi, Y.; Fang, R. P.; Ni, Z. F.; Shen, Y. C.; Ko, K.; Yamaguchi, I.; Isono, K. *J. Antibiot.* **1987**, *40*, 907–909.
(6) Cheng, X. C.; Ubukata, M.; Isono, K. *J. Antibiot.* **1990**, *43*, 890–896.
(7) Gupta, V.; Ogawa, A. K.; Du, X.; Houk, K. N.; Armstrong, R. W. *J. Med. Chem.* **1997**, *40*, 3199–3206.
(8) Liu, W.; Sheppeck, J. E., II; Colby, D. A.; Huang, H. -B.; Nairn, A. C.; Chamberlin, A. R. *Bioorg. Med. Chem. Lett.* **2003**, *13*, 1597–1600.

10.1021/ol900293j CCC: $40.75
Published on Web 03/12/2009

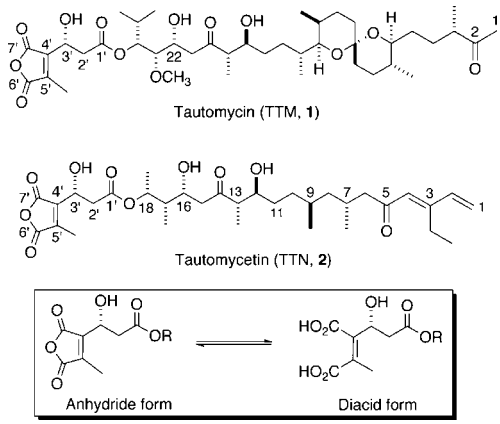

Figure 1. Structures of TTM (**1**) and TTN (**2**). The dialkylmaleic anhydride unit of both is involved in an equilibrium between closed anhydride form and ring-opened diacid form; the diacid form of each is the active PP inhibitor.[8,10]

PP-1 and PP-2A share significant sequence identity between their catalytic subunits (50% for residues 23−292; 43% overall) and are sensitive to a wide array of structurally diverse natural products;[7] **1** and **2** are unique due to their PP-1 selectivity. Although **1** potently inhibits PP-1 and PP-2A in weak preference to PP-1, **2** shows nearly 40-fold higher affinity for PP-1 (IC_{50} = 1.6 nM) than to PP-2A (IC_{50} = 62 nM).[2] This is remarkable in light of the high degree of structural similarity between PP-1 and PP-2A. Structural differences between **1** and **2**, distant from the crucial maleic anhydride (Figure 1), likely account for PP-1 selectivity.[8,9] This postulate is supported by the recently reported crystal structure of **1** bound to PP-1.[10] Further elucidation of PP inhibition by **1** and **2** promises to be facilitated not only by such structural biology efforts but also through the application of combinatorial biosynthetic methods and subsequent structure activity studies.

We recently cloned and sequenced the biosynthetic gene clusters for both **1** and **2**.[11,12] The *ttm* cluster was found to consist of twenty open reading frames that encode three modular type I polyketide synthases (TtmHIJ), one type II thioesterase (TtmT), five proteins for methoxymalonyl-S-acyl carrier protein biosynthesis (TtmABCDE), eight proteins for dialkylmaleic anhydride biosynthesis and regulation (TtmKLMNOPRS), as well as two additional regulatory proteins (TtmF and TtmQ) and one tailoring enzyme (TtmG).[11] A high degree of similarity between the *ttm* and *ttn* clusters was found, particularly among the genes related to dialkylmaleic anhydride synthesis.[11,12]

The overarching goal of this study was to functionally characterize the tailoring enzyme TtmM, a putative C3′ hydroxylase involved in biosynthesis of **1**. Here we report that: (i) inactivation of *ttmM* affords mutant strain SB6005 that accumulates three new C3′-deshydroxy TTM analogs in a fashion paralleling earlier studies of TTN biosynthesis;[12] (ii) loss of TtmM activity in the Δ*ttmM* mutant can be complemented by expressing a functional copy of *ttmM* in trans; (iii) removal of the 3′ OH moiety of **1** profoundly diminishes TTM biological activity; and (iv) PP inhibition is likely only one mechanism by which **1** and related analogs cause cell death.

Sequence analysis of the *ttm* cluster indicated that TtmM contains a conserved Fe(II)-α-ketoglutarate oxygenase (Fe(II)-2OG) domain.[13] Predicated on the similarity between TtmM and the Fe(II)-2OG oxygenases we envisioned *ttmM* as a putative C3′ oxygenase involved in biosynthesis of **1**.[11] Indeed, previous studies of TTN biosynthesis and the similarity between TtnM and TtmM supported this view.[12]

The oxygenase function of TtmM was confirmed by in vivo gene inactivation experiments exploiting *S. spiroverticillatus* mutant strain SB6005 in which the *ttmM* gene was removed using previously established methods (Supporting Information).[11,12] Genetic complementation to the Δ*ttmM* mutation in SB6005 was carried out in SB6010 by expressing a functional copy of *ttmM* in trans to eliminate the possibility of polar effects.

Fermentations of the Δ*ttmM* mutant strain SB6005, complemented strain SB6010 and wild-type strain were carried out and HPLC analyses conducted on each culture. Analysis of the SB6005 culture revealed the absence of intact **1**, which was clearly present in the wild type and SB6010 cultures (Figure 2A); the Δ*ttmM* mutation in SB6005 abolished production of **1** instead leading to the production of three new compounds, **3-5** (Figure 2A, II). All new compounds displayed UV−vis spectra identical to that of **1**, immediately suggesting retention of the dialkylmaleic anhydride moiety. Large scale fermentation of SB6005 permitted isolation of each new metabolite in quantities sufficient for complete structural characterization. The structures of **3-5** were determined on the basis of MS, 1D, and 2D NMR ($^1H-^1H$ COSY, TOCSY, HMQC, and gHMBC) spectroscopic data.

HRMALDIMS of **3** revealed a molecular formula of $C_{41}H_{66}O_{12}$, 16 mass units less than that of **1**, and consistent with a deshydroxy analog of **1**. The ^1H NMR spectrum of **3** revealed the absence of the C3′ ^1H resonance at 5.18 ppm ordinarily seen in **1**. Moreover, the ^{13}C NMR spectrum of **3**, revealed upfield shifting of the C3′ ^{13}C signal by 32.9 ppm, also consistent with the absence of oxygen connectivity at C3′. On the basis of 1D and 2D NMR (COSY, HMQC and gHMBC) spectra, all ^1H and ^{13}C signals of **3** were assigned (Table S1, Supporting Information). In the HMBC spectrum (Figure 2C), the signals due to H-2′, H-3′ and H-24 showed correlations to C-1′, further verifying that **3** lacks the C3′ OH group. Examination of other 1D and 2D NMR data revealed that **3** differed structurally from **1** only at the C3′ position, which lacks an OH group.

HRMALDIMS of **4** revealed a molecular formula of $C_{41}H_{68}O_{13}$, two mass units greater than that of **1**. ^{13}C and

(9) Colby, D. A.; Liu, W.; Sheppeck, J. E.; Huang, H. B.; Nairn, A. C.; Chamberlin, A. R. *Bioorg. Med. Chem. Lett.* **2003**, *13*, 1601–1605.
(10) Kelker, M. S.; Page, R.; Peti, W. *J. Mol. Biol.* **2009**, *385*, 11–21.
(11) Li, W.; Ju, J.; Rajski, S. R.; Osada, H.; Shen, B. *J. Biol. Chem.* **2008**, *283*, 28607–28617.
(12) Li, W.; Ju, J.; Rajski, S. R.; Osada, H.; Shen, B. *J. Nat. Prod.* **2009**, published ASAP, DOI: 10.1021/np8007478.

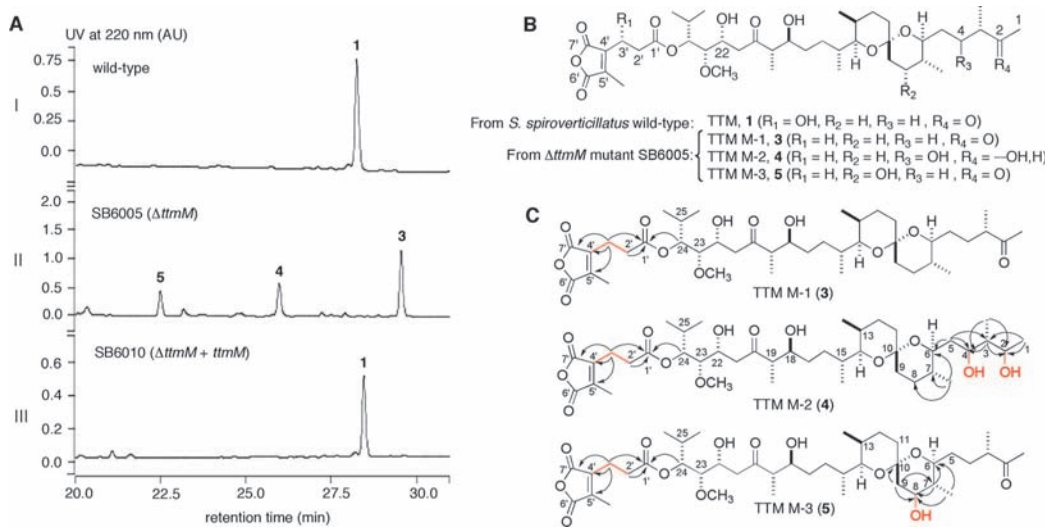

Figure 2. TTM analog production and structure elucidation. (A) HPLC analysis of Δ*ttmM* mutant strain SB6005 and complemented strain SB6010. (I) *S. spiroverticallitus* wild-type; (II) Δ*ttmM* mutant SB6005; (III) complemented strain SB6010. Numbers above HPLC peaks correspond to compounds **1**, **3**−**5**. (B) Structures of **1** and 3′-deshydroxy analogs **3**−**5** isolated from Δ*ttmM* mutant SB6005. (C) Selected HMBC correlations observed for **3**−**5** verify the absence of C3′ OH moiety in all three analogs and differentiate structural right hemisphere differences at C2, C4 and C8. New or modified functionalities (relative to **1**) are highlighted in red.

DEPT NMR spectroscopy showed the absence of the C3′ methine characteristic and the C2 ketone carbon ordinarily present in **1**. The carbonyl signal corresponding to C2 in **1** was absent in **4** although two new oxygenated methine signals at ∼75 ppm not found in **1** were detected in **4**. A full set of 1D and 2D NMR (COSY, TOCSY, HMQC and *g*HMBC) spectroscopic data of **4** were acquired, allowing full assignments of its ^{1}H and ^{13}C NMR signals (Table S1, Supporting Information). ^{1}H and ^{13}C NMR data suggest that **4**, like **3**, lacks the OH group found at C3′ of **1**. This was supported by HMBC correlations within the dialkylmaleic anhydride moiety attached to the C24 oxygen (Figure 2C). Detailed inspection of the ^{1}H and ^{13}C NMR data (Table S1, Supporting Information) suggested that **4** contained the same substructure through C-6 to C-27 and the same 2,3-dialkylmaleic anhydride moiety as found in **1**, which was supported by COSY and HMBC spectral analyses. Based on these spectroscopic findings and the molecular formula identified, **4** was proposed to be hydroxylated at C2 and C4. The methyl proton signal at C1 was observed as a doublet at δ 1.16 ppm (δ, $J = 7.5$ Hz), indicating the presence of a hydroxyl group at C2, which was substantiated by the observed HMBC correlation from H1 to C2 (Figure 2C). The other OH group was localized to C4 on the basis of HMBC correlations from H5 to C4 and C3, from H3 to C4, and from 3-CH_3 protons to C4.

HRMALDIMS of **5** established its molecular formula as $C_{41}H_{66}O_{13}$, the same as that of TTM. In order to clarify the structure difference between the two molecules, full 1D (^{1}H, ^{13}C and DEPT) and 2D (COSY, TOCSY, HMQC and *g*HMBC) NMR data sets were acquired, leading to complete accounting of all ^{1}H and ^{13}C NMR signals (Table S1, Supporting Information). Similar to **3** and **4**, **5** is devoid of the C3′ OH moiety, as evidenced by the absence of the C3′ methine proton at δ 5.18 ppm in the ^{1}H NMR spectrum and C3′ signal at δ 64.0 ppm in the ^{13}C NMR spectrum of **1**. HMBC correlations (Figure 2C) support this conclusion. Furthermore, comparative analyses of the ^{1}H and ^{13}C NMR data for **5** and **1** reveal that **5** bears C8 hydroxylation. Compared to data from **1**, the C8 signal in **5** was shifted downfield by 41.9 ppm, and the signals due to C-7 and C-9 were shifted downfield by 8.6 and 8.8 ppm, respectively, fully consistent with C8 hydroxylation of **5**. Additionally, ^{13}C NMR data for **5** showed the 7-CH_3 carbon signal to be shifted upfield by 5.0 ppm due to γ-gauche effect of the C8-substituent. The location of the hydroxyl group at C8 was further confirmed by HMBC correlations as shown in Figure 2C. Analysis of other 1D and 2D NMR data revealed that **5** shares the same C1−C6, C10−C27 and anhydride moiety substructures with **1**. Finally, the configuration of the 8-OH group was indicated by the significant 0.20 ppm downfield shift of the 7-CH_3 proton signals relative to **1**. The result of the syn-parallel relationship of the C8 OH and C7 CH_3 substituents, the observed downfield shift is consistent with an *R* stereochemical configuration at the C8 position. Emphasis on the 8-OH to 7-CH_3 relationship to determine C8 stereochemistry stemmed from the complexity and overlapping of other signals with those of H-7 and H-8; the coupling constant for H-7 and H-8 could not be readily deciphered (Figure S5, Supporting Information). Moreover, the application of NOE experiments was of little use due to the cyclic nature of C8 and C7 and well established limitations of NOE in elucidating 1,2 proton relationships within such cyclic systems.

Production of **3**−**5** exclusively in SB6005 but not in either wild-type or SB6010 strains confirms that TtmM, like TtnM in TTN biosynthesis, serves a vital role as a C3′ hydroxylase.[12] That fermentation of SB6005 yields, not one, but three new analogs of **1** has important implications for TTM biosynthesis and for combinatorial biosynthetic strategies to new TTM analogs. As depicted in Figure 2B, **4** possesses

the same right hemisphere as **1** but lacks the C2 ketone of **1** instead bearing hydroxylation at both C2 and C4. TTM M-3 (**5**) retains the C2 ketone of **1** but possesses an OH moiety at C8. Neither **4** or **5** are produced by *S. spiroverticillatus* wild-type strain and the production of **3**-**5**, instead of only 3′-deshydroxy-TTM (**3**) suggests that C3′ hydroxylation by TtmM likely proceeds early during the synthesis of **1**. This is reminiscent of findings related to biosynthesis of **2** wherein the Δ*ttnM* mutant strain accumulated four new compounds, none of which are synthesized by *S. griseochromogenes* wild-type strain.[12] Once envisioned to occur in a completely convergent manner where anhydride and polyketide units for both **1** and **2** were independently synthesized and coupled at a very late stage (following release of the full length polyketide intermediate from the corresponding synthase), these new findings support a linear pathway calling for anhydride-to-polyketide coupling prior to polyketide release from the polyketide synthase.[11,12]

Coupling of the 3′-deshydroxy anhydride moiety to the TTM polyketide during chain extension appears to present TTM polyketide synthase with inefficient substrates. Such poor substrates provide a rationale for the diversity of products accumulated by Δ*ttmM* mutant SB6005. Specific structural features of both **4** and **5** can be rationalized on the basis of TTM polyketide synthase domain organization.[11] Specifically, we envision the OH moieties at C4 and C8 of **4** and **5**, to result from the impaired ability of DH domains in modules 11 and 9, respectively, to process 3′-deshydroxy substrates as efficiently as the natural TTM precursors. Although the origin of the C2 OH in **4** is not readily apparent based on current knowledge of TTM biosynthesis this functionality is likely not introduced until after polyketide release from the polyketide synthase; a late stage decarboxylation calls for the presence of a β-ketoacid capped polyketide.[11] However, the C4 OH may enhance the ability of a C2 ketone to undergo adventitious reduction en route to **4** via provision of an intramolecular H-bonding motif.

The recently solved crystal structure of **1** bound to PP-1 has revealed critical determinants for PP-1 binding by the diacid form of **1**.[10] Among these, the C3′ OH moiety forms an H-bond with the amide NH of Val250. Previous studies showing C3′ *epi*-TTM to be ~1000 fold less effective at PP-1 inhibition than **1** have shown the clear importance C3′ stereochemistry but not necessarily its mere presence.[8] Hence, production of **3** permitted us to examine this issue. We evaluated the cytotoxicity of **1** and **3**-**5** against A549 lung adenocarcinoma, Du145 colon carcinoma, HT29 colon adenocarcinoma and MCF7 breast carcinoma cell lines (Table 1). Additionally, we evaluated the activity of **1** and its congeners as inhibitors of PP-1 and PP-2A (Table 2).

The results of cytotoxicity and PP inhibition assays for **1**, **3**, **4**, and **5** shed new insight into the relationship of PP inhibition to cell killing capacity for these compounds. All 3′-deshydroxy TTM analogs were found to be approximately 1 order of magnitude less cytotoxic than **1** (Table 1) invoking the clear significance of the C3′ OH moiety. Consistent with previous reports, **1** was much more effective at inhibiting PP-1 than PP-2A (Table 2) and did so at low nM concentrations.[1,2,8] More surprising was that all three 3′-deshydroxy analogs are very poor inhibitors of both PPs. PP-1 could be inhibited by **3**-**5** but with IC_{50} values 1000-fold higher than for **1**, consistent with earlier studies of C3′ *epi*-TTM.[8]

Table 1. Summary of Cytotoxicity Data (IC_{50} in μM) for TTM (**1**) and Its Analogs (**3**, **4**, and **5**) against Established Cell Lines[a]

compound	A549	Du145	HT29	MCF7
1	1.66 ± 0.14	nd	0.59 ± 0.01	1.8 ± 0.12
3	26.6 ± 6.4	4.24 ± 0.11	7.35 ± 0.19	15.6 ± 0.90
4	nd	26.5 ± 1.05	27.3 ± 3.9	nd
5	16.4 ± 1.14	20.0 ± 1.7	32.0 ± 2.22	9.30 ± 0.57

[a] nd, not detected.

Table 2. Summary of IC_{50} Values (nM) for TTM (**1**) and Its Analogs (**3**, **4**, and **5**) from PP Inhibition Assays[a]

	PP-1		PP-2A	
compound	pH 7.5	pH 8.4	pH 7.5	pH 8.4
1	0.58	0.86	15.0	42.6
3	470	677	15635	15269
4	2614	5056	110510	69938
5	382	1277	20136	66576

[a] PP inhibition assays were conducted at pH 7.5 and 8.4 because the anhydride-diacid equilibrium is known to favor the active diacid form at pH > 8.[14] Assays performed in triplicate prior to IC_{50} determination (Supporting Information).

The significantly greater impact of C3′ OH removal upon PP inhibition than on cytotoxicity, relative to **1**, makes clear that PP inhibition is not the sole means by which TTM exerts antitumor activity. This is consistent with previous reports of apoptosis induction by **1**, which is independent of PP inhibition and relies on structural determinants separate from those needed for PP inhibition.[4] This realization and our full knowledge of the *ttm* biosynthetic gene cluster[11] provides a framework for future biosynthetic and mechanistic studies of **1**.

Acknowledgment. We thank the Analytical Instrumentation Center of the School of Pharmacy, UW-Madison for support in obtaining MS and NMR data. This work is supported in part by NIH grants CA113297.

Supporting Information Available: Detailed experimental procedures, ^{1}H and ^{13}C NMR spectra and spectral data for compounds **3**−**5**, and PP inhibition curves for compounds **1**, and **3**−**5**. This material is available free of charge via the Internet at http://pubs.acs.org.

OL900293J

(13) Clifton, I. J.; McDonough, M. A.; Ehrismann, D.; Kershaw, N. J.; Granatino, N.; Schofield, C. J. *J. Inorg. Biochem.* **2006**, *100*, 644–669.
(14) Sugiyama, Y.; Ohtani, I. I.; Isobe, M.; Takai, A.; Ubukata, M.; Isono, K. *Bioorg. Med. Chem. Lett.* **1996**, *6*, 3–8.